Mode Conversion to the Kinetic Alfvén Wave in Low-Frequency Heating Experiments in the TCA Tokamak

H. Weisen, K. Appert, G. G. Borg, B. Joye, A. J. Knight, J. B. Lister, and J. Vaclavik

Centre de Recherches en Physique des Plasmas, Association Euratom-Confédération Suisse, Ecole Polytechnique Fédérale de Lausanne, 21, Avenue des Bains, CH-1007 Lausanne, Switzerland

(Received 11 April 1989)

Excitation of Alfvén waves in the TCA tokamak using an external antenna structure produces a radially inward propagating and strongly damped wave which is observable through its associated density oscillations. It is found to have the properties of the kinetic Alfvén wave predicted to be created by resonant mode conversion at shear Alfvén wave resonance layers. Our experimental results are compared with the original theory of Hasegawa and Chen and with numerical calculations in cylindrical geometry.

PACS numbers: 52.50.Gj, 52.35.−g

Resonant absorption of radio-frequency power at the local Alfvén resonance as a means of plasma heating was proposed by Grossmann and Tataronis[1] as well as Hasegawa and Chen.[2] The latter formulated a kinetic description in planar geometry at high temperatures where the electron thermal velocity (v_e) is greater than the Alfvén speed (V_A). This theory predicts that an externally applied low-frequency ($\omega < \omega_{ci}$) oscillating field is mode converted at the Alfvén resonance layer to a short-wavelength wave that propagates towards the plasma interior. The short-wavelength mode is referred to as the kinetic Alfvén wave (KAW).[2,3] The subject was further developed by Stix,[4] Ross, Chen, and Mahajan,[5] Donnelly, Clancy, and Cramer,[6] and Appert *et al.*[7] The latter three provided numerical kinetic calculations of the wave fields in cylindrical geometry.

The experiments have been carried out in the TCA tokamak with major radius $R = 0.61$ m, minor radius $A = 0.18$ m, and toroidal magnetic field $B_\phi = 1.5$ T. A plasma current of 130 kA gives the safety factor at the limiter radius $q(a) \sim 3$. The antenna structure consists of eight groups of six poloidal current-carrying bars. The eight groups occur in top and bottom pairs spaced at 90° intervals in the toroidal direction. Each group is fed separately so that the toroidal wave number (n) can be determined by their relative phasings. A detailed description of experiments on plasma coupling to Alfvén waves for the purpose of Alfvén wave heating, a more detailed presentation of the theory, and an extensive bibliography are presented by Collins *et al.*[8]

An Alfvén resonance is excited whenever the local Alfvén velocity V_A matches the externally imposed wave velocity $\omega/k_\parallel$. In the large-aspect-ratio approximation this condition can be written as

$$\omega^2\rho(r) = [n + m/q(r)]^2 (B_T^2/\mu_0 R^2)(1 - \omega^2/\omega_{ci}^2), \quad (1)$$

where ρ is the mass density, q is the safety factor, m is the poloidal mode number, and B_T is the total magnetic field. In this approximation the toroidal field is constant but B_T varies slightly with radius as a result of its dependence on the poloidal field at finite plasma current. Since the KAW is excited at the Alfvén resonance layer defined by Eq. (1) a radial profile of its wave field can be used to measure $q(r)$ and hence the current profile.[9] Figure 1(a) shows the resonance position as a function of the central density for two sets of mode numbers considered here, $(n,m) = (2,0)$ and $(-1,-1)$, with $B_T = 1.5$ T in a deuterium plasma, as relevant to our experimental conditions. The density profile was modeled to be parabolic and the current profile of the form $j(r) = j(0)(1 - r^2/a^2)^{2.2}$ such that $q(0) = 1$ and $q(a) = 3.2$. The flatness of the $(-1,-1)$ resonance curve results from its dependence on the safety factor profile. Our choice of $q(0) = 1$ for the modeled profile is dictated by our observation that $(\pm 1, \pm 1)$ and (2,0) resonances are excited in the plasma core at the same density and frequency.[9]

To detect the density modulations associated with the electrostatic component of the KAW an imaging diagnostic based on the phase contrast method was installed on TCA.[10] It is similar to a laser imaging interferometer and is equipped with a thirty-element HgCdTe infrared detector array and mixer detection for sixteen channels.

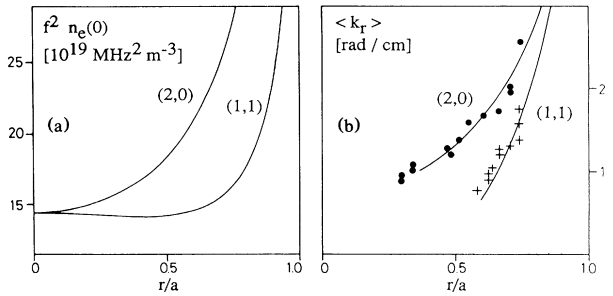

FIG. 1. (a) Resonance position as a function of frequency and central density for modeled mass density and current profiles. (b) Mean radial wave number as a function of position (averaged over one cycle of propagation). The solid lines are obtained from the KAW dispersion relation.

It provides simultaneous measurement of the amplitude and phase of the line integral of the density fluctuations at sixteen different locations between $r/a=0$ and $r/a\cong 0.8$. Because of the approximate cylindrical symmetry of the waves, the pattern of the line integrated-density perturbation remains closely related to the original radial wave pattern. To a first approximation the local amplitude is multiplied by an effective integration length $L_{\text{eff}}=(2\pi r/k_r)^{0.5}$, where k_r is the radial wave number of the wave.

It is an accepted procedure, when identifying an experimentally detected plasma wave or mode, to show that it obeys the expected theoretical dispersion relation. A straightforward application of this procedure in the context of resonant mode conversion is difficult because the local wave number (the spatial derivative of the wave phase) varies rapidly from zero to a finite value as the wave propagates away from the resonance position. In Fig. 1(b) we have instead plotted the average wave number $\langle k_r\rangle$ over the first cycle of inward propagation as a function of the position of the amplitude maximum. The solid lines were obtained from the approximate dispersion relation for the KAW expressed as

$$k_r^2\rho_i^2(\tfrac{3}{4}+T_e/T_i)=(\omega^2-k_\parallel^2V_A^2)/k_\parallel^2V_A^2, \qquad (2)$$

where ρ_i is the ion Larmor radius. Although this relation is only valid for a homogeneous plasma, the k_r obtained by replacing V_A^2 by a linearly position-dependent V_A^2 about the resonance layer agrees well with the wavelength predicted by Hasegawa and Chen's original calculation[3] for a linear density profile. In this simple comparison we therefore choose to avoid more complicated dispersion relations which take better account of the profiles of density and plasma current. An example of such a dispersion relation would be that of Mahajan;[11] however, his neglect of finite Larmor radius renders the comparison invalid. The resonance profiles from Fig. 1(a) were used together with a combined temperature profile $T_e+\frac{3}{4}T_i$ assumed to be a parabola squared with a central value of 1 keV, in accordance with temperature measurements on TCA. Again $\langle k_r\rangle$ is an average over the first cycle and is plotted as a function of resonance position. The further the resonance layers are from the plasma center, the larger is $\langle k_r\rangle$ as a result of both the decreased temperature and the steepening of the resonance curves. The smaller $\langle k_r\rangle$ for $(-1,-1)$ is a result of the shallowness of the $(-1,-1)$ resonance profile. These waves remain closer to resonance and therefore maintain a longer wavelength. Propagating waves with wave numbers significantly smaller than indicated in Fig. 1(b) are not observed. Closer to the thresholds only standing waves occur.

Figure 2 shows examples of radial profiles of the amplitude and phase of the driven density fluctuations at different line densities with $(n,m)=(-1,-1)$ and (2,0), and $P_{\text{rf}}\approx 40$ kW at 2 MHz. For $(n,m)=(-1,-1)$ the antennas were phased to produce a toroidally propagating wave, whereas the (2,0) was excited via toroidal coupling by a (2,1) antenna structure.

At densities near the threshold below which the resonances are not in the plasma, the oscillations have the character of standing waves (constant phase profiles except for jumps of π). Standing waves result when (a) Eq. (1) is satisfied at more than one radius so that KAW's mode converted at these radii can interfere or, (b) Eq. (1) is satisfied near the plasma axis so that the inward propagating KAW can interfere with itself after reflection from the axis. At higher densities neither of these conditions is satisfied. In this case the KAW has a mainly propagating character (sloping phase profiles), with wavelengths that become shorter as the resonance layers move away from the plasma center. The onset of propagating waves with increasing central plasma density is clearly dependent on the radial damping. We restrict this paper to the discussion of propagating waves because they bear the closest relation to Hasegawa and Chen's original KAW model that can be expected in the finite geometry of a tokamak. As a consequence, we are excluding the global Alfvén eigenmodes[12,13] from the study since these can only exist in the vicinity of the Alfvén continuum threshold.

Depending on collisionality, the damping of the KAW can be dominated either by collisional damping or by Landau damping. In the region accessible to observation in the TCA tokamak, the KAW is predicted to be strongly electron Landau damped. Electron heating in the plasma core has been observed near the thresholds of the $(n,m)=(2,0)$ and (2,1) resonances under nonstationary conditions of increasing plasma density.[14] Localized off-axis heating above the thresholds, however, has not been observed.[15] The fractional damping rate $\delta_{eL}=\frac{1}{2}\pi^{1/2}V_A/v_e$ is in the range 0.2 (near the plasma center where $T_e\approx 800$ eV) to 0.5 for a $(-1,-1)$ KAW near $r/a=0.7$, where $T_e\approx 200$ eV. This is in good agreement with our observation that the amplitude e-folding lengths estimated inward from the amplitude maxima are about one wavelength in the core region, but can be as small as 0.4 of a wavelength near $r/a=0.7$. The fractional collisional damping rate $\delta_{ec}=\omega\nu_{ei}k_\parallel^{-2}v_e^{-2}$ is an order of magnitude or more below δ_{eL} for the conditions of the experiment for $T_e\geq 200$ eV, but may play an important role in the edge plasma. Our data show no evidence for a significant reduction of the Landau damping rate by trapped electrons as suggested in Hasegawa and Chen's original work.[2,3] Nonlinear effects are not expected at our levels of perturbation ($\tilde{n}_e/n_e\sim 10^{-3}$–$5\times 10^{-3}$). We have also verified that the detected wave amplitude scales linearly with antenna current over 1 order of magnitude in current, corresponding to radio-frequency powers of up to 100 kW.

In Fig. 3 we show examples of numerically calculated wave fields using the ISMENE kinetic code.[7,16] It solves a

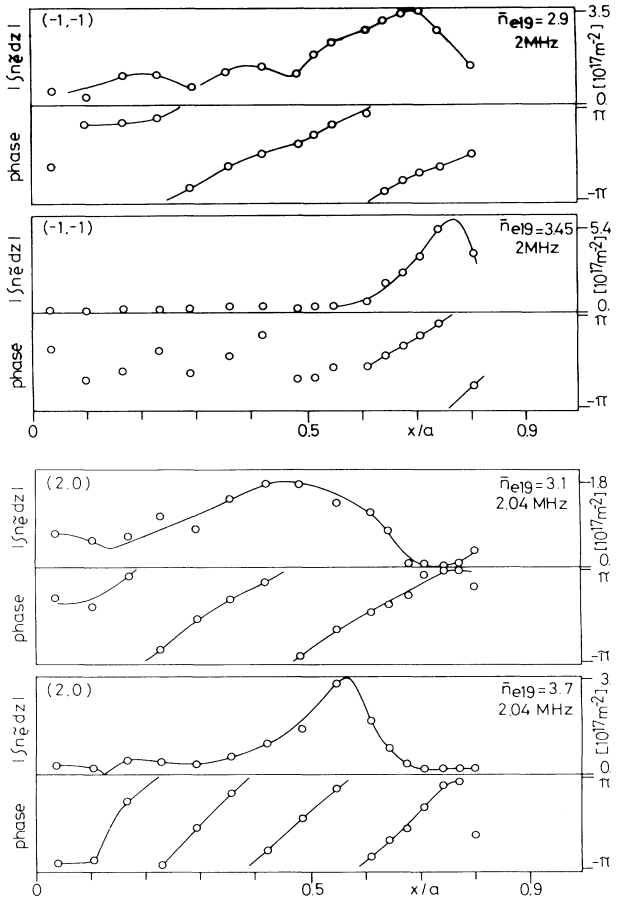

FIG. 2. Examples of observed profiles of line density fluctuations in the $(-1,-1)$ and (2,0) continua.

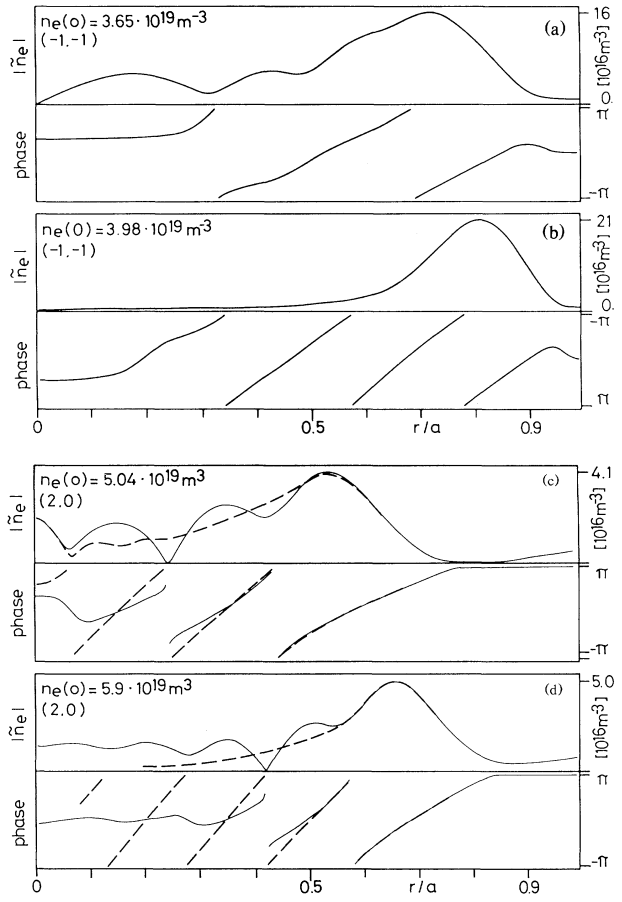

FIG. 3. Examples of calculated density fluctuations in the $(-1,-1)$ and (2,0) continua. The resonance layer positions were chosen to match those of Fig. 2. The broken lines of (c) and (d) for the (2,0) KAW represent the remaining wave field after subtraction of the fast-wave mode.

sixth-order ordinary differential equation and includes Landau damping, transit-time magnetic pumping, certain equilibrium gradient terms, and uses the formulation of Vaclavik and Appert[17] for the local power absorption. The profiles of plasma parameters were as for Fig. 1(a).

Although there is a striking similarity between the wave fields observed and predicted by kinetic theory, exact matching of the two should not be expected because (a) we have compared the line-integrated density fluctuation from the experiment with the point function density from the code and (b) the details of the wave fields depend sensitively on the profiles of plasma parameters which are only coarsely modeled in the code. The general features of the wave fields, however, are insensitive to details in the plasma profiles. Absolute amplitudes for a given power agree within a factor of 2. In the case of $(n,m) = (2,0)$ direct excitation is poor. As a result the KAW amplitude in Figs. 3(c) and 3(d) is not much larger than the fast-wave amplitude from which it mode converts. The profiles are therefore not representative of those obtained in a tokamak where (2,0) waves are excited efficiently by a (2,1) antenna structure as a result of toroidal coupling.[18] The experimental results should therefore be compared with the wave profiles shown as broken lines, where the fast wave has been subtracted to obtain the (2,0) KAW component.

In conclusion, we have observed and identified the kinetic Alfvén wave resulting from linear mode conversion at the shear Alfvén wave resonance layers. Our experimental results agree with the KAW dispersion relation and the observed wave fields are accurately modeled by our kinetic calculations. The attenuation of the wave amplitude is consistent with electron Landau damping.

We would like to acknowledge stimulating discussions with Professor F. Troyon, Dr. Liu Chen, and Dr. Akira Hasegawa, as well as the support of our colleagues of the TCA team and technical staff. This work was partly supported by the Swiss National Science Foundation.

[1]W. Grossmann and J. Tataronis, Z. Phys. **261**, 217 (1973).
[2]A. Hasegawa and L. Chen, Phys. Rev. Lett. **35**, 370 (1975).

[3]A. Hasegawa and L. Chen, Phys. Fluids **19**, 1924 (1976).

[4]T. H. Stix, in *Proceedings of the Second International Symposium on Heating in Toroidal Plasmas, II, Como, Italy, 1980,* edited by E. Canobbio *et al.*, (Commission of the European Communities, Brussels, Belgium, 1980), Vol. II, p. 631.

[5]D. W. Ross, G. L. Chen, and S. M. Mahajan, Phys. Fluids **25**, 652 (1982).

[6]I. J. Donnelly, B. E. Clancy, and N. F. Cramer, J. Plasma Phys. **35**, 75 (1986).

[7]K. Appert *et al.*, in *Proceedings of the International Conference on Plasma Physics, Kiev, U.S.S.R., 1987,* edited by A. Sitenko (World Scientific, Singapore, 1987), Vol. 2, p. 1230.

[8]G. A. Collins *et al.*, Phys. Fluids **29**, 2260 (1986).

[9]H. Weisen *et al.*, Phys. Rev. Lett. **62**, 434 (1989).

[10]H. Weisen, Rev. Sci. Instrum **59**, 1544 (1988).

[11]S. M. Mahajan, Phys. Fluids **27**, 2238 (1984).

[12]K. Appert, R. Gruber, F. Troyon, and J. Vaclavik, Plasma Phys. **24**, 1147 (1982).

[13]S. M. Mahajan, D. W. Ross, and G. L. Chen, Phys. Fluids **26**, 2195 (1983).

[14]B. Joye *et al.*, Phys. Rev. Lett. **56**, 2481 (1986).

[15]J.-M. Moret, Ph.D. thesis, 1988, Centre de Recherches en Physique des Plasmas, Ecole Polytechnique Fédérale de Lausane Report No. CRPP-EPFL 358/88 (unpublished).

[16]Th. Martin and J. Vaclavik, Helv. Phys. Acta **60**, 471 (1987).

[17]J. Vaclavik and K. Appert, Plasma Phys. Contr. Fusion **29**, 257 (1987).

[18]K. Appert *et al.*, Phys. Rev. Lett. **54**, 1671 (1985).